Solvation Dynamics of Fluorophores with an Anthroyloxy Group at the Heptane/Water Interface as Studied by Time-Resolved Total Internal Reflection Fluorescence Spectroscopy

Tomohisa Yamashita, Tatsuya Uchida,[†] Takanori Fukushima,[‡] and Norio Teramae*

Department of Chemistry, Graduate School of Science, Tohoku University, Aoba-ku, Sendai 980-8578, Japan

Received: May 23, 2002; In Final Form: December 30, 2002

Solvent relaxation processes of 12-(9-anthroyloxy) stearic acid (12-AS) and 4-(9-anthroyloxy) butanoic acid (4-ABA) at the heptane/water interface are examined by time-resolved total internal reflection fluorescence spectroscopy. In a bulk heptane solution containing 3 M ethanol, both 12-AS and 4-ABA show time-dependent fluorescence spectral shifts, and the decay profiles can be analyzed by the two-state kinetics model. The results obtained for the binary mixture of heptane and ethanol can be ascribed to a local enrichment of ethanol molecules around fluorophores, that is, preferential solvation. A similar result is obtained for 12-AS but not for 4-ABA at the heptane/water interface, indicating that the preferential solvation occurs for 12-AS at the heptane/water interface. Since 4-ABA does not show a time-dependent spectral shift at the interface, the fluorophore of 4-ABA is surrounded by more water molecules, by which quenching of fluoresence was accelerated, than 12-AS at the heptane/water interface, and it is located more closely to the water phase than 12-AS.

Introduction

The chemical processes occurring at the interface between two immiscible liquids are well-known to play an important role in many fields such as separation chemistry and biochemistry.[1,2] Various analytical techniques have been applied to reveal characteristics of liquid/liquid interfaces. In particular, linear and nonlinear laser spectroscopies represented by time-resolved total internal reflection (TIR) fluorescence,[3−5] and second harmonic generation (SHG)[6−8] spectrocopies have been used to obtain information on liquid/liquid interfaces on a microscopic level. In these spectroscopies, molecules sensitive to the microenvironment are usually used to probe characteristic parameters of liquid/liquid interfaces such as polarity[3,4,7] and interfacial roughness.[9] As for the polarity of liquid/liquid interfaces, its value has been reported to be intermediate between those of the organic and aqueous phases based on the measurements by attenuated total internal reflectance,[10] TIR fluorescence,[3,4] and SHG[7] spectroscopies, and these experimental results agree well with the prediction by molecular dynamics simulations.[11] Despite these extensive studies on liquid/liquid interfaces by laser spectroscopies, experimental studies on solvation dynamics at liquid/liquid interfaces have not been reported yet except for the molecular dynamics simulations.[12,13]

As for the solvent relaxation process in bulk media, the process is known to be completed within several tens of picoseconds in an isotropic bulk medium composed of a singular solvent.[14] In binary solvent systems such as cyclohexane−ethanol, it has been reported that the solvent relaxation of 2-aminonaphthalene occurs in a time scale of a few hundred picoseconds.[15] The solvent relaxation has also been reported to occur in a time scale ranging from a few hundred picoseconds to nanoseconds in viscous ordered media[16] having structural heterogeneities such as micelles, reverse micelles, vesicles, and cyclodextrins. Since the solvent relaxation process depends on the properties of media where fluorescent probe molecules locate, it is expected that characteristic solvent relaxation processes will be observed at liquid/liquid interfaces; hence, results different from the relaxation processes observed in bulk solvent systems are beneficial to obtain deeper understanding of liquid/liquid interfaces.

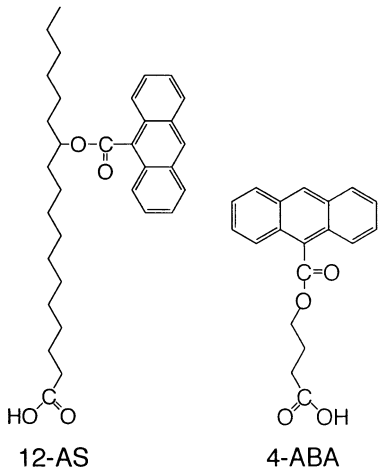

Figure 1. Molecular structures of 12-(9-anthroyloxy) stearic acid (12-AS) and 4-(9-anthroyloxy) butanoic acid (4-ABA).

In the present study, time-resolved TIR fluorescence spectra are examined using fluorescent molecules (Figure 1) to probe solvation dynamics at the heptane/water interface. In Figure 1, both 12-(9-anthroyloxy) stearic acid (12-AS) and 4-(9-anthroyloxy) butanoic acid (4-ABA) have an anthroyloxy group as a fluorophore, which is sensitive to the change in solvated environments because the fluorophore has strong charge-transfer character in the excited state.[17−20] In addition, solubilities of

* To whom correspondence should be addressed. E-mail: tera@anal.chem.tohoku.ac.jp.

[†] Present address: School of Life Science, Tokyo University of Pharmacy and Life Science, Hachioji 192-0392, Japan.

[‡] Present address: ERATO Nanospace Project, JST, National Museum of Emerging Science and Innovation, 2-41 Aomi, Koto-ku, Tokyo 135-0064, Japan.

10.1021/jp026163m CCC: $25.00
Published on Web 04/11/2003

12-AS and 4-ABA in heptane or water differ from each other; the former is easily dissolved in heptane, and the latter in water. Thus, it is also interesting to examine the effect of the difference in affinity for heptane or water on solvation dynamics at the heptane/water interface.

Experimental Section

Chemicals. Water was doubly distilled and deionized with a milli-Q Labo system (Millipore Co.). 12-AS (Molecular Probes Inc.), heptane (Nakarai Tesque Inc.), sodium dihydrogen phosphate dihydrate (Wako Pure Chemical Industries Ltd.), and sodium hydrogen phosphate (Wako Pure Chemical Industries Ltd.) were used without further purification. 4-ABA was newly synthesized, and the synthetic procedure is described at the end of the text.

Sample Preparation. As sample solutions for TIR fluorescence measurements, heptane was poured carefully onto an aqueous solution of 2×10^{-2} M sodium phosphate buffer in a sample cell. pH of the aqueous solution was kept at 7.0. Concentrations of probe molecules were as follows: [12-AS] $= 1 \times 10^{-8}$ M in heptane, [4-ABA] $= 5 \times 10^{-6}$ M in a phosphate buffer solution.

Measurement. The experimental setup for the time-resolved fluorescence spectroscopy was described in detail previously. The measurement system was composed of a mode-locked Ti:sapphire laser (Spectra-Physics, Tsunami 3960; ca. 100 fs at 780 nm, 82 MHz) pumped by an Ar^+ laser (Spectra-Physics, Model 2060), a polychromator (Hamamatsu, C5094), and a streak scope (Hamamatsu, C4334). The repetition rate of the Ti:sapphire laser was reduced to 4 MHz with an electrooptic modulator (Spectra-Physics, Model 3980), and the second harmonic of the Ti:sapphire beam generated by an LBO crystal (Spectra-physics, GWU) was used as an excitation source. The maximum time-resolution of the present system was approximately 60 ps at 5 ns full scale.

In the TIR fluorescence measurement, the excitation laser beam, polarized perpendicular to the plane of incidence (s-polarized), was introduced through the heptane phase to the heptane/water interface with an incident angle of 77°, which was sufficiently larger than the critical angle of 73.5° for total reflection. The interfacial fluorescence was collected perpendicular to the interface and focused on the polychromator slit.

To obtain fluorescence arising from the interface, extraneous emission from the heptane phase has to be eliminated from the streak image measured by the TIR method, since 12-AS is dissolved in heptane and 4-ABA dissolved in the aqueous buffer solution can distribute to the heptane phase. Thus, additional measurements were carried out by moving the collecting optics to obtain the fluorescence only from the heptane phase; the data thus obtained were used for subtraction procedures of streak images to obtain fluorescence from the interface. 12-AS and 4-ABA in heptane have fluorescence lifetimes of 7.76 and 9.19 ns, respectively. Thus, subtraction procedures of streak images were assured of nonappearance of such lifetime components in fluorescence from the interface.

12-AS is hardly dissolved in the aqueous phase at pH 7.0, and fluorescence of 12-AS in the aqueous phase was not detected using an optical arrangement of 90 degree scattering. The distribution ratio of 12-AS from heptane to water (pH 7.0) is less than 0.0001, which was determined by absorption and fluorescence measurements. Though the distribution ratio of 4-ABA from water (pH 7.0) to heptane is 0.021, the lifetime of of 4-ABA at the heptane/water interface (1.14 ns) is different from that of 4-ABA in heptane (9.19 ns). The lifetime of 4-ABA in the aqueous phase is ca. 300 ps.

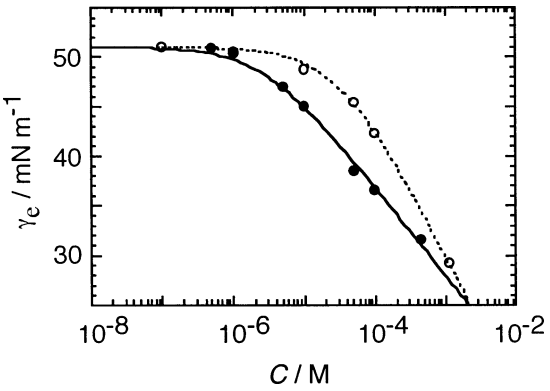

Figure 2. Probe concentration dependence of interfacial tension at the heptane/water interface: 12-AS (●) and 4-ABA(○).

The interfacial tension at the heptane/water interface was measured by a dynamic drop volume method[21] in the presence or absence of probe molecules to estimate their interfacial concentrations. All measurements were carried out at 298 ±0.5 K.

Results and Discussion

Adsorption of 12-AS or 4-ABA to the Heptane/Water Interface. Figure 2 shows the dependence of the equilibrium interfacial tension at the heptane/water interface on the concentration of 12-AS or 4-ABA. The equilibrium interfacial tension γ_e decreases upon addition of 12-AS or 4-ABA as the concentration of solutes increases. The decrease in the equilibrium interfacial tension is ascribed to the adsorption of solutes to the heptane/water interface. The plots of γ_e can be analyzed by the Gibbs adsorption isotherm by which the equilibrium interfacial excess Γ_e of solutes can be expressed as follows:[21]

$$\Gamma_e = -\frac{1}{2.303RT}(\partial\gamma_e/\partial \log C)_T \qquad (1)$$

where C, R, and T denote the concentration of solute, gas constant, and absolute temperature, respectively. By fitting the plotted data in Figure 2 with eq 1, interfacial concentrations of 12-AS and 4-ABA can be estimated as 6.15×10^{-13} and 3.09×10^{-11} mol cm^{-2} for the concentrations of 1×10^{-8} M of 12-AS and 5×10^{-6} M of 4-ABA, respectively. From these results, interaction between probe molecules at the heptane/water interface can be considered to be negligible, and fluorescence behavior observed at the heptane/water interface reflects the microenvironment of the probe molecules.

Dynamic Behavior of Probe Molecules at the Heptane/Water Interface. Both 12-AS and 4-ABA have an anthroyloxy group as a fluorophore, and the emission wavelength of the anthroyloxy group is known to depend on the solvent polarity.[17] These probe molecules show emission maxima at ca. 460 nm in heptane and at ca. 480 nm in methanol. The fact that both molecules show the same emission wavelengths in solvents with different polarities indicates that fluorescence characteristics of these molecules are governed mainly by the anthroyloxy group irrespective of other groups included in the probe molecule. Figure 3 shows fluorescence spectra of 12-AS and 4-ABA at the heptane/water interface and in heptane or an aqueous phosphate buffer solution (pH 7.0). Spectra a−c were measured in a time window of 0−4.5 ns after pulsed excitation, and a time window of 0−1.0 ns was used for spectrum d because of the short fluorescence lifetime of 4-ABA in an aqueous solution.

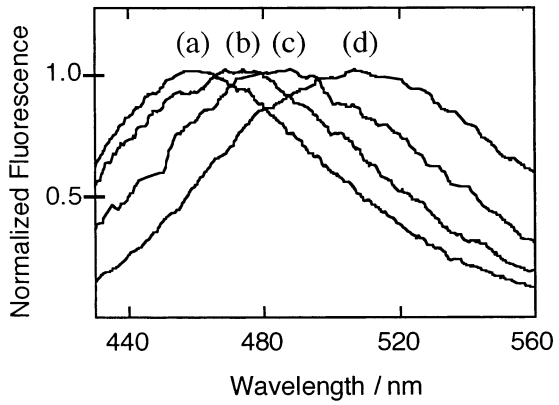

Figure 3. Fluorescence spectra of 12-AS and 4-ABA. (a) 1×10^{-5} M 12-AS in heptane. (b)12-AS at the heptane/water interface, [12-AS] = 1×10^{-8} M in heptane. (c) 4-ABA at the heptane/water interface, [4-ABA] = 5×10^{-6} M in phosphate buffer (pH 7.0). (d) 1×10^{-5} M 4-ABA in aqueous phosphate buffer (pH 7.0).

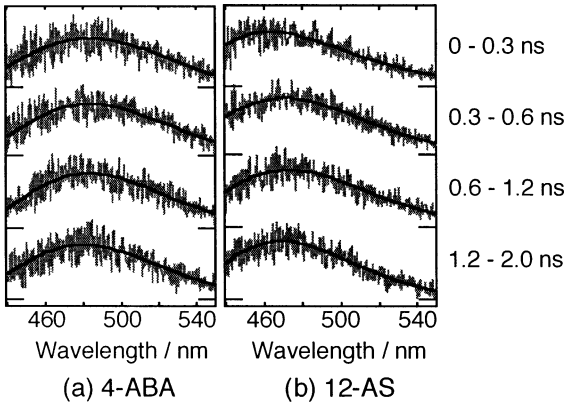

Figure 4. Time-dependent fluorescence spectra of 12-AS and 4-ABA at the heptane/water interface for four time windows. (a) [12-AS] = 1×10^{-8} M in heptane. (b) [4-ABA] = 5×10^{-6} M in phosphate buffer (pH 7.0).

The emission maximum of 12-AS in heptane is observed at ca. 460 nm (Figure 3a) and that of 4-ABA in an aqueous phosphate buffer solution is observed at ca. 505 nm (Figure 3d). The emission maxima of 12-AS and 4-ABA at the heptane/water interface appear in the wavelength region between those of 12-AS in heptane and 4-ABA in an aqueous phosphate buffer solution as shown in Figure 3b,c. This result indicates that the polarity of the heptane/water interface has an intermediate value between the polarities of heptane and water. It is noted that the wavelengths of fluorescence maxima of 12-AS and 4-ABA at the heptane/water interface differ from each other, and 4-ABA exhibits a red-shifted peak in comparison with 12-AS. This difference means that 4-ABA is in an environment with higher polarity at the heptane/water interface compared with 12-AS. Accordingly, it can be said that the solvation environment surrounding the fluorophore at the heptane/water interface depends on the structure of probe molecules, even if they have the same anthroyloxy group fluorophore.

To obtain detailed information on solvation, time-resolved fluorescence spectra of 4-ABA and 12-AS were measured at the heptane/water interface, and the results are shown in Figure 4 by dividing into four time windows. As seen in Figure 4a, 4-ABA shows the same emission wavelength at ca. 480 nm in all time windows. In contrast, 12-AS (Figure 4b) shows time-dependent spectral shift to red as the time window increases. The fluorescence maximum of 12-AS is observed at ca. 465 nm in the time window of 0−0.3 ns just after excitation. As time passes, the fluorescence maximum wavelength shifts to red, and is observed at ca. 475 nm in the time window of 1.2−2.0 ns. As a cause of this time-dependent spectral shift, either intramolecular rotational relaxation[22] or solvent relaxation[15,23,24] is considered. The former process is usually completed within a few picoseconds except in media with high viscosity. Since 4-ABA does not show any time-dependent spectral shift (Figure 4a), it can be said that the viscosity of the heptane/water interface is not so high and that the intramolecular rotational relaxation should be completed within the time-resolution of the present measurement system. Thus, the solvent relaxation process seems a plausible cause for the time-dependent spectral shift observed for 12-AS at the heptane/water interface.

TABLE 1: Fluorescence Decay Parameters for 12-AS at the Heptane/Water Interface for Three Different Wavelength Regions

	lifetime (ns)		pre-exponential factor[a]	
wavelength (nm)	τ_1	τ_2	α_1	α_2
455−515	1.91	0.33	0.83	0.27
470−550	1.83			
515−600	1.81	0.33	1.97	-0.97

[a] Normalized to $\alpha_1 + \alpha_2 = 1$.

TIR fluorescence decay curves of 4-ABA and 12-AS were examined by dividing the fluorescence spectral region into three wavelength regions, that is, short (455−515 nm), long (515−600 nm), and crossover (470−550 nm) wavelength regions. In the case of 4-ABA, TIR fluorescence decay curves can be fitted by a single-exponential function irrespective of wavelength regions, and the fluorescence lifetime is 1.14 ns. In contrast, the TIR fluorescence decay curve of 12-AS at the heptane/water interface varies according to the fitting wavelength region as shown in Figure 5. In both the short and long wavelength regions, decay curves can be fitted by double exponential functions expressed by

$$F(t) = \alpha_1 \exp\left(-\frac{t}{\tau_1}\right) + \alpha_2 \exp\left(-\frac{t}{\tau_2}\right) \qquad (2)$$

where $F(t)$ denotes a decay curve in a specified wavelength region and α_1 and α_2 are preexponential coefficients. τ_1 and τ_2 are fluorescence lifetimes. In the crossover wavelength region, the decay curve can be fitted by a single-exponential function. Table 1 summarizes the estimated lifetime and preexponential coefficient values. As listed in Table 1, both long-lifetime (τ_1) and short-lifetime (τ_2) are independent of the emission wavelength region, and they are about 1.8 and 0.3 ns, respectively.

In the study on solvation dynamics in a binary mixture of polar and nonpolar solvents, dynamic fluorescence behavior depending on wavelength regions was reported,[15] and these results are similar to those shown in Figure 5 and Table 1. According to the previous study,[15] fluorescence of 12-AS at the heptane/water interface can be analyzed by the two-state kinetics model,[25] which is schematically illustrated in Scheme 1, where E_G is the ground state, E_I is the initial state, and E_R is the relaxed state stabilized by solvation. τ_I and τ_R are lifetimes of the initial and the relaxed states, respectively. k is the solvent relaxation rate constant from the initial state to the relaxed state. A probe molecule is excited to the initial state by photoexcitation, and thereafter, it relaxes from the initial state to the relaxed state. Emission occurs at different wavelengths from both the initial and relaxed states. In the initial period, fluorescence appears at the shorter wavelength, and then appears at the longer wavelength in the process of solvent relaxation. On the basis of the two-state kinetics model, fluorescence decay

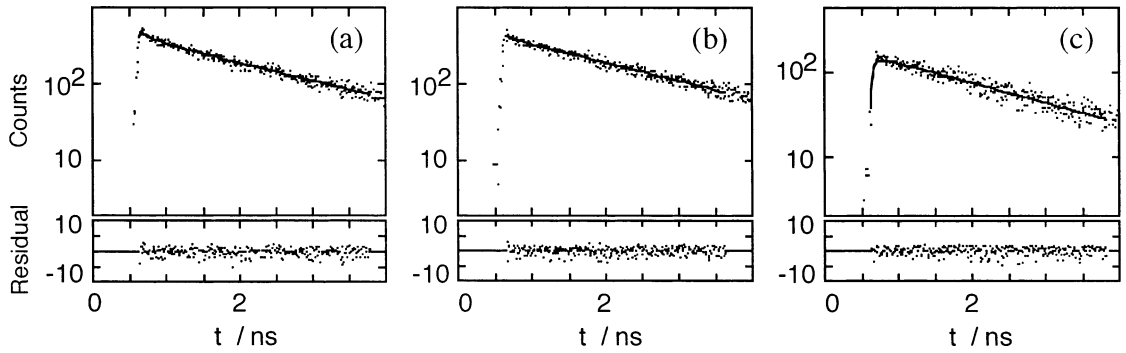

Figure 5. Fluorescence decay profiles of 12-AS at the heptane/water for three different wavelength regions: (a) 455−515, (b) 470−550, and (c) 515−600 nm.

SCHEME 1: Schematic Representation of the Two-State Kinetics Model for Solvent Relaxation

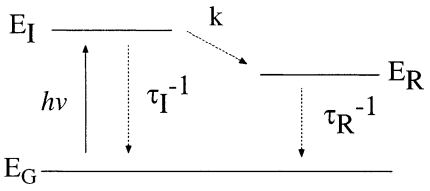

curves are expressed by the following equation[25] which is obtained by rewriting eq 2:

$$F(t) = (\alpha_I - \alpha_R)\exp\left\{-\left(k + \frac{t}{\tau_I}\right)t\right\} + \alpha_R \exp\left\{-\left(\frac{t}{\tau_R}\right)\right\} \quad (3)$$

where $F(t)$ is the fluorescence intensity as a function of time t in a given wavelength region and α_I and α_R are fluorescence contributions from the initial and relaxed states, respectively. In the short-wavelength region corresponding to the initial period, α_I is larger than α_R, and the fluorescence decay curve is described by double exponential functions. In the long-wavelength region corresponding to the relaxed period, α_I becomes smaller than α_R, and the fluorescence decay curve is also described by double exponential functions with a negative preexponential coefficient for the short-lifetime component. In the crossover-wavelength region, the fluorescence decay curve is described by a single-exponential function when $\alpha_I = \alpha_R$. The parameters listed in Table 1 agree well with the expectations deduced from the two-state kinetics model. The lifetimes of τ_1 and τ_2 in Table 1 correspond to τ_R and $\{k + (1/\tau_I)\}^{-1}$ in eq 3, respectively.[25]

As for solvation dynamics in bulk solutions, it has been reported that solvent relaxation time in a binary mixture of polar and nonpolar solvents varies from several tens of picoseconds to nanoseconds, depending on the mixing ratio of polar and nonpolar solvents.[15,23,24,26] Detoma and Brand[15] analyzed solvation dynamics of 2-anilinonaphthalene (2-AN) in cyclohexane containing 0.1 M ethanol on the basis of the two-state kinetics model, and they reported that the time-dependent spectral shift was completed within a few hundred picoseconds. To obtain more information on solvation dynamics of 12-AS and 4-ABA at the heptane/water interface, solvation dynamics of these probe molecules were examined in a binary mixture of polar and nonpolar solvents. Figure 6 shows time-resolved fluorescence spectra of 4-ABA and 12-AS in heptane containing 3 M ethanol. The time-dependent spectral shift is easily recognized for both 4-ABA and 12-AS. Fluorescence decay profiles of 4-ABA and 12-AS are shown in Figures 7 and 8, respectively; the profiles vary with the wavelength region.

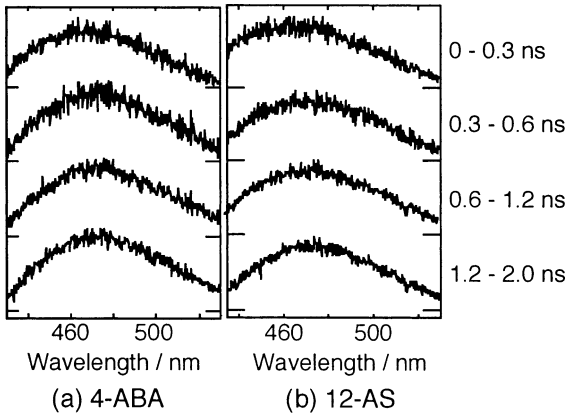

Figure 6. Time-dependent fluorescence spectra of 4-ABA and 12-AS in heptane containing 3 M ethanol for four time windows. (a) [4-ABA] $= 5 \times 10^{-6}$ M. (b)[12-AS] $= 5 \times 10^{-5}$ M.

Decay curves were analyzed using eq 2 to obtain lifetimes and preexponential coefficients. In the short-wavelength region (420−450 nm), the decay curves can be fitted by double-exponential functions. In the long-wavelength region (500−580 nm), the decay curves can also be fitted by double exponential functions, but the preexponential coefficients of a short-lifetime component are negative. In the crossover wavelength region (455−480 nm), the decay curves can be fitted by a single-exponential function. Estimated values are summarized in Table 2. As listed in Table 2, the values of long-lifetime (τ_1) and short-lifetime (τ_2) are independent of the wavelength regions for 12-AS and 4-ABA. These results are characteristics of the two-state kinetics model and are similar to dynamic behavior observed for 12-AS at the heptane/water interface. Comparison of the lifetimes of 12-AS listed in Tables 1 and 2 indicates that the short-lifetime components are close to each other. On the other hand, the long-lifetime component (ca. 5 ns) for 12-AS in the mixed solvent (Table 2) is larger than that obtained at the heptane/water interface (2 ns; Table 1). This difference in the long-lifetime component can be ascribed to the fact that the degree of fluorescence quenching depends on the hydrogen bonding ability of solvents. It is known that the fluorescence of the anthroyloxy group is quenched by hydrogen bond formation in a protic solvent.[27] Accordingly, the above-mentioned difference in the long-lifetime component of fluorescence suggests that the anthroyloxy group of 12-AS is surrounded by more protic solvent molecules, that is, water, in the excited state at the heptane/water interface in contrast to the binary mixture of heptane and ethanol.

From the above discussions based on the two-state kinetics model, the anthroyloxy group of 12-AS at the heptane/water interface is considered to be solvated by more heptane molecules

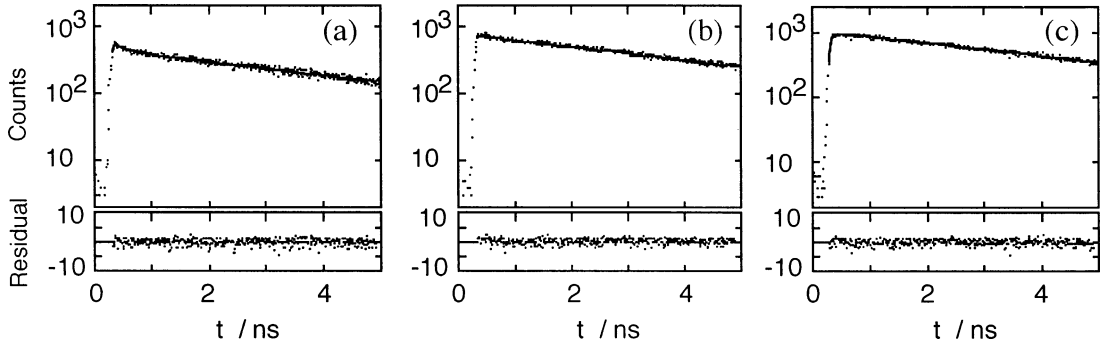

Figure 7. Fluorescence decay profiles of 4-ABA in heptane containing 3 M ethanol for three different wavelength regions: (a) 420−450, (b) 455−480, and (c) 500−580 nm.

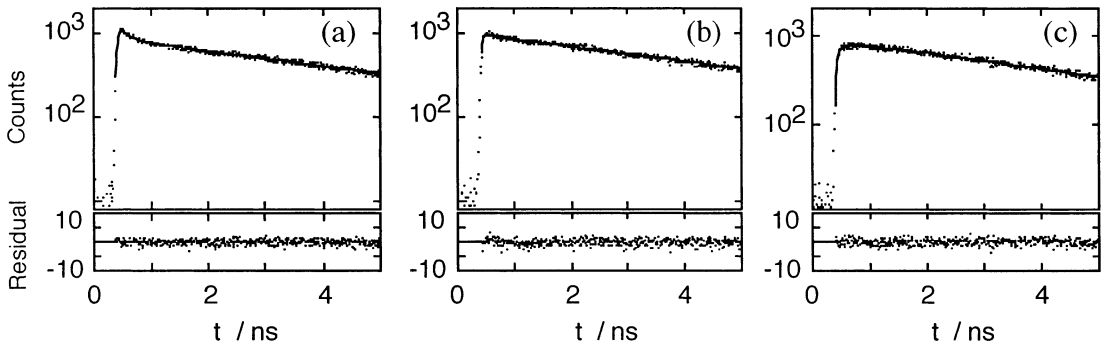

Figure 8. Fluorescence decay profiles of 12-AS in heptane containing 3 M ethanol for three different wavelength regions: (a) 420−450, (b) 455−480, and (c) 500−580 nm.

TABLE 2: Fluorescence Decay Parameters for 4-ABA and 12-AS in Heptane Containing 3 M Ethanol for Three Different Wavelength Regions

	lifetime (ns)		pre-exponential factor[a]	
wavelength (nm)	τ_1	τ_2	α_1	α_2
		4-ABA		
420−450	4.29	0.18	0.72	0.28
455−480	4.29			
500−580	4.36	0.18	1.23	−0.23
		12-AS		
420−450	4.93	0.24	0.71	0.29
455−480	4.83			
500−580	4.91	0.25	1.31	−0.31

[a] Normalized to $\alpha_1 + \alpha_2 = 1$.

in the ground state, and intramolecular charge-transfer occurs within the anthroyloxy group after excitation and its dipole moment increases in the excited state. This increase in the dipole moment induces rearrangement of solvent molecules in the solvent shell surrounding the anthroyloxy group, and this rearrangement results in the increase in the number of water molecules adjoining the fluorophore, which is called "preferential solvation".[26] This is the cause of the time-dependent spectral shift observed at the heptane/water interface.

The emission maximum of the time-dependent spectrum, $\upsilon_m(t)$, can be assumed to shift to lower energy in an exponetial fashion with a solvent relaxation time τ_s and is expressed by the following equation:[26,28]

$$\upsilon_m(t) = (\upsilon_m(0) - \upsilon_m(\infty))\, e^{-t/\tau_s} + \upsilon_m(\infty) \qquad (4)$$

where $\upsilon_m(0)$ and $\upsilon_m(\infty)$ represent the emission maxima of the initially excited and relaxed states, respectively. The fluorescence frequency maxima of 12-AS and 4-ABA in heptane containing 3M ethanol and at the heptane/water interface were plotted against time and the results were shown in Figures 9 and 10, respectively. These plots can be fitted by eq 4 and the estimated parameters ($\upsilon_m(0)$, $\upsilon_m(\infty)$, and τ_s) are summarized in Table 3. As can be seen from Figure 9 and Table 3, the solvent relaxation times of 12-AS and 4-ABA are almost identical in heptane containing 3 M ethanol. In contrast, difference in the solvent relaxation time between 12-AS and 4-ABA is remarkable at the heptane/water interface as shown in Figure 10. This result indicates that the solvent relaxation for 4-ABA is very fast at the heptane/water interface. This fast relaxation is ascribed to the large number of water molecules surrounding the fluorophore of 4-ABA compared with 12-AS. The solvent relaxation time of 12-AS is 0.27 ns at the hepatane/water

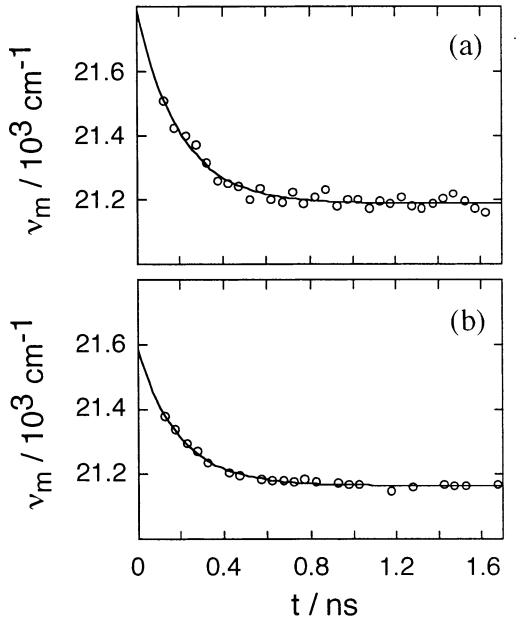

Figure 9. Fluorescence frequency maximum vs time for (a) 12-AS and (b) 4-ABA in heptane containing 3 M ethanol.

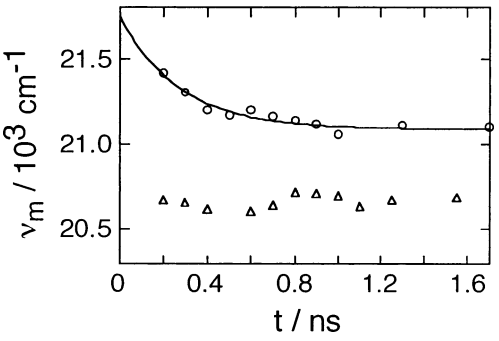

Figure 10. Fluorescence frequency maximum vs time for 12-AS (o) and 4-ABA(Δ) at the heptane/water interface.

TABLE 3: Decay Parameters of Probe Molecules (a) at the Heptane/Water Interface and (b) in Heptane Containing 3 M Ethanol

	$\nu_m(0)$, cm^{-1}	$\nu_m(\infty)$, cm^{-1}	τ_s, ns
	(a) Heptane/Water		
12-AS	21750	21090	0.27
	(b) Heptane with Ethanol		
12-AS	21790	21190	0.20
4-ABA	21580	21170	0.19

interface (Table 3), though 12-AS does not show any time-dependent spectral shift in heptane. This indicates that the solvent relaxation at the interface occurs more slowly than in the bulk solution, which is similar to the case of coumarin dye at liquid−solid interface layer.[29] In simulations by molecular dynamics, Michael and Benjamin[13] reported that solvent relaxation of a solute located on the organic side of the interface is slow compared with a solute at the Gibbs surface because of the slow diffusion of water molecules. According to this simulation, the anthroyloxy group of 12-AS is considered to locate on the heptane side from the interface compared with that of 4-ABA, and it is also concluded that the location of probe molecule is an important factor for understanding solvation dynamics at liquid/liquid interfaces.

Conclusion

This is first experimental study on solvation dynamics at the liquid/liquid interface, and it was concluded that preferential solvation occurred for 12-AS at the heptane/water interface based on observation of time-dependent fluorescence spectral shift and analysis using the two-state kinetics model. Although both 12-AS and 4-ABA showed time-dependent fluorescence spectral shift in a binary mixture of nonpolar and polar solvents, 4-ABA did not show preferential solvation at the heptane/water interface within the time-resolution of the present measurement system. This fact meant that 4-ABA was surrounded by more water molecules, by which quenching of fluorescence was accelerated, than 12-AS at the haptane/water interface, and it was located more closely to the water phase than 12-AS. It was also found that the solvent relaxation of 12-AS at the interface occurred more slowly than in the bulk solution system. A further study including molecular dynamics simulation should reveal detailed characteristics of liquid/liquid interfaces and afford deeper understanding of chemical reactions at them.

Synthesis of 4-(9-Anthroyloxy) Butanoic Acid (1)

A mixture of anthracene-9-carboxylic acid (1.11 g, 5 mmol), thionyl chloride (0.45 mL, 6.2 mmol), and dimethyl formamide (0.04 mL) in dry dichloromethane (10 mL) was stirred for 0.5 h at room temperature and then refluxed for another 4 h. Upon evaporation of the solvent, anthracene-9-carbonyl chloride **2** was obtained as yellow residue, which was used without further purification.

1,4-Butanediol (4.5 g, 50 mmol), dry pyridine (1 mL), and **2** were dissolved in dry dichloromethane (30 mL). The reaction solution was stirred at room temperature for 15 h under nitrogen atmosphere, followed by washing with water several times. The organic phase was washed with brine and dried over Na_2SO_4, and then the solvent was evaporated. Purification by silica gel chromatography with dichloromethane-diethyl ether (10:1) as eluent gave the 4-(9-anthroyloxy) butanol **3** as yellow oil (1.26 g, 85 %). Analysis: ^{1}H NMR (270 MHz, $CDCl_3$) δ(ppm) 8.52 (s, 1H), 8.02 (m, 4H), 7.50 (m, 4H), 4.65 (t, J = 8.9 Hz, 2H), 3.72 (d, J = 6.5 Hz, 2H), 1.99 (t, J = 10.1 Hz, 2H), 1.74 (m, 2H), 1.39 (s, 1H).

A suspension of sulfur trioxide pyridine complex (1.43 g, 9 mmol) in dry dimethyl sulfoxide (10 mL) was added to a dry dichloromethane solution of **3** (0.082 g, 3.0 mmol) and triethylamine (3 mL, 21 mmol) under nitrogen atmosphere. The mixture was stirred for 1 h at room temperature, and then water and diethyl ether were added. The organic phase was successively washed with aqueous ammonium chloride, aqueous sodium hydrogen carbonate, water, and brine before being dried over Na_2SO_4. Evaporation of the solvent gave the 4-(9-anthroyloxy) butanal **4** as yellow oil, which was used without further purification.

Sodium chlorite (0.17 g, 1.9 mmol) was added to a mixture of 2-methyl-2-butene (0.32 g, 4.6 mmol), potassium dihydrogen phosphate (0.069 g, 0.5 mmol), water (1 mL), *tert*-butyl alcohol (4 mL), and **4**. The mixture was stirred for 1 h at room temperature and cooled at 0°, then adjusted to pH 1 with 1 M hydrochloric acid. After dichloromethane was added to the reaction mixture, and the organic phase was washed with acidic brine, dried over Na_2SO_4, and evaporated to give yellow oil. The yellow oil was purified by silica gel chromatography with dichloromethane-diethyl ether (3:1) as eluent to give yellow residue. The residue was further purified by recrystallization from the mixture of dichloromethane and hexane, giving **1** as yellow crystals. Analysis: ^{1}H NMR (270 MHz, $CDCl_3$) δ(ppm) 8.52 (s, 1H), 8.02 (m, 4H), 7.50 (m, 4H), 4.66 (t, J = 8.4 Hz, 2H), 2.55 (t, J = 9.7 Hz, 2H), 2.19 (m, 2H). MS (m/z): calcd. for M^+, 308; found, M^+ 308. Anal. Calcd. for $C_{19}H_{16}O_4$: C, 74.01 H, 5.23%; found, C, 74.07 H, 5.35%.

Acknowledgment. This work was supported by Grants-in-Aid for Scientific Research on Priority Areas, No. 13129201 from the Ministry of Education, Science and Culture, Japan, and by Grants-in-Aid for Scientific Research (A), No. 14204074 from the Japan Society for the Promotion of Science.

References and Notes

(1) Volkov, A. G.; Deamer, D. W.; Tanelian, D. L.; Martin, V. S. *Liquid Interface in Chemistry and Biology*; John Wiley & Sons: New York, 1998.

(2) Volkov, A. G.; Deamer, D. W. *Liquid-Liquid Interfaces − Theory and Methods*; CRC Press: New York, 1996.

(3) Bessho, K.; Uchida, T.; Yamauchi, A.; Shioya, T.; Teramae, N. *Chem. Phys. Lett.* **1997**, *264*, 381.

(4) Ishizaka, S.; Kim, H.-B.; Kitamura, N. *Anal. Chem.* **2001**, *73*, 2421.

(5) Ishizaka, S.; Kitamura, N. *Bull. Chem. Soc. Jpn.* **2001**, *74*, 1983.

(6) Corn, R. M.; Higgins, D. A. *Chem. Rev.* **1994**, *94*, 107.

(7) Wang, H.; Borguet, E.; Eisenthal, K. B. *J. Phys. Chem. B* **1998**, *102*, 4927.

(8) Uchida, T.; Yamaguchi, A.; Ina, T.; Teramae, N. *J. Phys. Chem. B* **2000**, *104*, 12091.

(9) Ishizaka, S.; Habuchi, S.; Kim, H.-B.; Kitamura, N. *Anal. Chem.* **1999**, *71*, 3382.

(10) Perera, J. M.; Stevens, G. W.; Grieser, F. G. *Colloids Surf. A: Physicochem. Eng. Aspects* **1995**, *95*, 185.
(11) Michael, D.; Benjamin, I. *J. Chem. Phys.* **1997**, *107*, 5684.
(12) Benjamin, I. *Chem. Rev.* **1996**, *96*, 1449.
(13) Michael, D.; Benjamin, I. *J. Chem. Phys.* **2001**, *114*, 2817.
(14) Maroncelli, M.; Macinnis, J.; Fleming, G. R. *Science* **1989**, *243*, 1674.
(15) Detoma, R. P.; Brand, L. *Chem. Phys. Lett.* **1977**, *47*, 231.
(16) Nandi, N.; Bhattacharyya, K.; Bagchi, B. *Chem. Rev.* **2000**, *100*, 2013.
(17) Garrison, M. D.; Doh, L. M.; Potts, R. O.; Abraham, W. *Chem. Phys. Lipids* **1994**, *70*, 155.
(18) Werner, T. C.; Hercules, D. M. *J. Phys. Chem.* **1969**, *73*, 2005.
(19) Werner, T. C.; Hoffman, R. M. *J. Phys. Chem.* **1973**, *77*, 1611.
(20) Werner, T. C.; Matthews, T.; Soller, B. *J. Phys. Chem.* **1976**, *80*, 533.
(21) Shioya, T.; Nishizawa, S.; Teramae, N. *Langmuir* **1998**, *14*, 4552.
(22) Berberan-Santos, M. N.; Prieto, M. J. E.; Szabo, A. G. *J. Phys. Chem.* **1991**, *95*, 5471.
(23) Petrov, N. Kh.; Wiessner, A.; Fiebig, T.; Staerk, H. *Chem. Phys. Lett.* **1995**, *241*, 127.
(24) Petrov, N. Kh.; Wiessner, A.; Staerk, H. *J. Chem. Phys.* **1998**, *108*, 2326.
(25) Lakowics, J. R. *Principle of Fluorescence Spectroscopy*; Plenum Press: New York, 1983.
(26) Cichos, F.; Willert, A.; Rampel, U.; Borczyskowski, C. *J. Phys. Chem. A* **1997**, *101*, 8179.
(27) Macanita, A. L.; Costa, F. P.; Costa, S. M. B.; Melo, E. C.; Santos, H. *J. Phys. Chem.* **1989**, *93*, 336.
(28) Mazurenko, Yu. T.; Bakhshiev, N. K. *Opt. Spectrosc.* **1970**, *28*, 490.
(29) Yanagimachi, M. T.; Tamai, N.; Masuhara, H. *Chem. Phys. Lett.* **1992**, *200*, 469.